Met. Mater. Int., Vol. 23, No. 3 (2017), pp. 444~449
doi: 10.1007/s12540-017-6399-0

Effects of Tensile Twinning on the Stretch Formability of Mg

Joong Won Park, Sang Jun Park, and Kwang Seon Shin*

Magnesium Technology Innovation Center, Research Institute of Advanced Materials
School of Materials Science and Engineering, Seoul National University, Seoul 08826, Republic of Korea

(received date: 8 June 2016 / accepted date: 6 October 2016)

This study examined the influences of twinning during the Erichsen test. {10-12} tensile twinning plays the critical role in Mg alloys. Alloy elements and grain size are important factors that determine the formation of {10-12} tensile twins at room temperature. Mg-6.0Zn(Z6) and Mg-6.0Zn-0.3Ca(ZX60) alloys were fabricated and their grain size was varied under different annealing conditions. Tensile twinning is promoted by the addition of Ca, as assessed from measurements of the microstructure and the viscoplastic self-consistent calculations. The coarse-grain Ca-containing alloy showed the largest amount of tensile twinning. However, the stretch formability increased with grain size up to a certain point and then decreased. It can be inferred that microstructures with large grains activated the tensile twin, which became origins of cracks. The results of the small Erichsen test showed that tensile twinning contributes to high stretch formability releasing the stress concentration in the grain boundaries but the interaction between twin and slip causes cracks as the grain size increases.

Keywords: rolling, twinning, erichsen test, alloying elements, grain size

1. INTRODUCTION

The difficulty in forming Mg wrought alloys at room temperature arises from its lack of deformation mode at room temperature. The addition of alloy elements, such as rare earth (RE) elements, Y, and Ca, has been considered widely as a way to overcome this limitation. Some of these introduce alloying elements may promote non-basal slip and satisfy the von Mises criterion, which requires a minimum of five independent slip modes [1-3]. Other studies suggest that the high formability and ductility are associated with the prevalence of tensile twinning, which may enhance strain accommodation among the grains by releasing the stress concentration during deformation [3-5].

Ca is one of the most promising alloying elements to enhance the stretch formability because of its relatively low cost as are placement for RE elements. The addition of Ca was also reported to weaken the basal texture [6-8]. Although Ca solute atoms have been reported widely, the element enhances the stretch formability at room temperature, but the mechanism is not completely understood. Several studies have examined the mechanism: activating non-basal slip mode [2,3] or tensile twin mode during deformation at room temperature [5,9].

The role of Ca addition is difficult to determine because the initial microstructure (grain size, texture, and alloy content etc.) affects the stretch formability and tensile twinning [10-12]. Therefore, minimizing the influence from the microstructure is essential. A 50% reduction ratio and 250 °C rolling temperature were determined when rolled Mg-Zn and Mg-Zn-Ca alloys were fabricated because a high strain strengthens the typical basal texture [13]. To consider the grain size effects, four different grain sizes were produced by varying annealing conditions. To compare the two alloy sets, electron back scattered diffraction (EBSD), optical microstructure analysis, and X-ray diffraction (XRD) were employed after the Erichsen tests. The small Erichsen test was newly designed to determine the role of tensile twinning during the Erichsen tests.

2. EXPERIMENTAL PROCEDURE

The materials were prepared by extrusion with 2 nominal compositions of Z6 and ZX60 followed by hot rolling. The specimens were preheated at 250 °C for 20 min before rolling. Rolling was performed with a rolling reduction of 50% per pass until a thickness of 1 mm was obtained using 200 °C hot rolls. The annealing conditions were changed to prepare specimens with four different grain sizes: annealing temperature of 250 °C for 1 h and annealing temperature of 350 °C for 1 h, 24 h, and 48 h.

The textures were measured by X-ray diffraction (XRD, PANalytical X'Pert PRO) using a Cu Kα source. The pole figures were obtained from the normal direction planes of the rolled sheets and the data were calculated using the arbitrarily defined

*Corresponding author: ksshin@snu.ac.kr

cells (ADC) method with LaboTex 3.0 software [14].

The microstructures and textures were examined by EBSD using field emission scanning electron microscopy (FE-SEM, SU-70, HITACHI) fitted with a TSL EBSD camera operating at 20 kV, and a 70° tilting angle. The specimens were prepared by mechanical polishing using sand papers and alumina powder followed by chemical etching with acetic – picral (4.2 g picric acid, 10 ml acetic acid, 10 ml H_2O, and 70 ml ethyl alcohol). Data with a confidence index >0.1 were used for texture and twin analysis.

The tensile specimens with a 20 mm gauge length, 4 mm gauge width, and 1 mm thickness were machined from rolled alloys. The tensile tests with a loading in the rolling direction were carried out at room temperature with a nominal strain rate of 2×10^{-4} s^{-1}. The Erichsen tests were carried out using a hemispherical punch with a diameter of 20 mm and a 5 mm/min punch speed. Each condition was assessed 3 times and the average was used for further analysis.

3. RESULTS AND DISCUSSION

The microstructures and (0002) basal pole figures were obtained from the ND planes of the two Z6 alloys. All the microstructures had recrystallized grain structures with equiaxial grains and grain sizes distributed homogeneously in Fig. 1(a)-(f). The grain sizes of Z6 and ZX60 alloys changed from 6.0 to 121.3 μm and from 5.8 to 93.2 μm, respectively, with four different annealing temperatures and times. In particular, changing the annealing temperature of 250 °C to 350 °C increased the grain size considerably; the grain size increased from 6.0 to 58.3 μm. On the other hand, the grain growth rate in ZX60 alloys was slower than that in Z6; the grain size of ZX60 increased from 5.8 to 35.8 μm with increasing annealing temperature. The basal pole figures of the two alloys were aligned approximately parallel to the normal direction. The maximum basal pole peaks appear in the normal direction and spread slightly towards the rolling direction. The Ca-containing alloy exhibits slightly lower basal pole intensity.

Erichsen tests were conducted on the two Z6 alloys with various grain size conditions to minimize the effects of the grain size on the stretch formability, as shown in Fig. 1(g). All the IE values as a function of the grain size showed a similar tendency; they increased and then decreased. The IE values of the ZX60 alloys were higher than Z6. Moreover, the points where the curves began to decrease differ according to the alloys. The ZX60 alloys showed the peak stretch formability

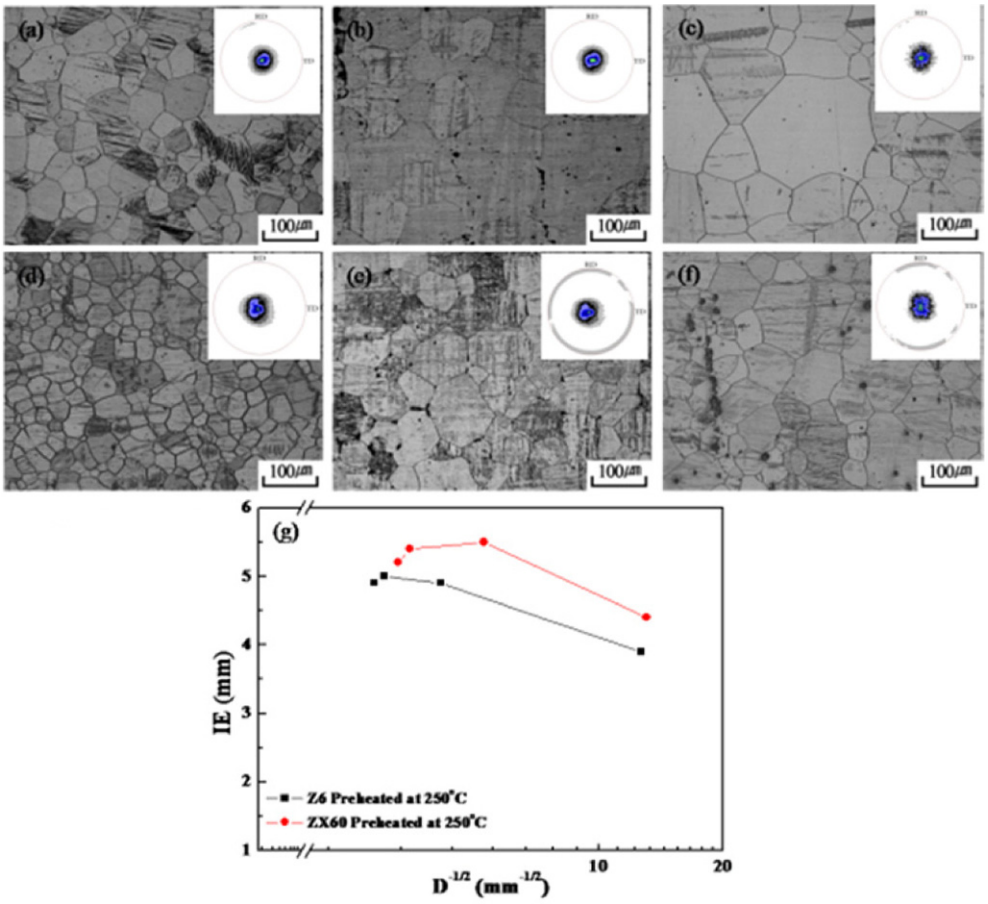

Fig. 1. Evolution of the microstructures and textures obtained from the ND planes of Z6 annealed at 350 °C for 1 h, 24 h, and 48 h (a, b, c) and ZX60 annealed at 350 °C for 1 h, 24 h, 48 h (d, e, f), and IE value as a function of the grain size (g).

at smaller grain sizes than the Z6 alloys, which indicates that the grain size affects the mechanical properties differently.

The Ca-containing alloy exhibited lightly weaker basal texture and a lower grain growth rate. The textures and microstructures were affected by the processing conditions, such as the rolling temperature, strain rate, and alloy compositions. Various single crystal studies and viscoplastic self-consistent (VPSC) calculations have shown that the critical resolved shear stress (CRSS) of the non-basal slip systems decrease with the addition of Li [1,3]. Moreover, Y-, RE-, and Ca-containing alloys exhibited texture weakening during thermo-mechanical processing, such as rolling and extrusion [1,2,6,13,15,16]. Tensile twinning can form a strong basal texture while activating non-basal slip modes, which leads to deformation in the c-axis, can suppress the twinning at high temperatures and help weaken the basal texture [13,17]. Therefore, the addition of Ca, contributes to the weak basal texture promoting the activation of non-basal slip instead of tensile twinning.

The mechanical properties are associated with the relative activation of deformation modes. Based on the results of the uniaxial tensile and compressive tests, the VPSC model was applied to analyze the effects of the grain size on the deformation modes: Basal slip {0001} <11$\bar{2}$0>, prismatic slip {10$\bar{1}$0} <11$\bar{2}$0>, pyramidal slip {11$\bar{2}$2} <11$\bar{2}$3>, and tensile twin {10$\bar{1}$2} <10$\bar{1}$1>.The CRSS values of the four deformation modes were calculated in the two Z6 alloys with various grain sizes, and

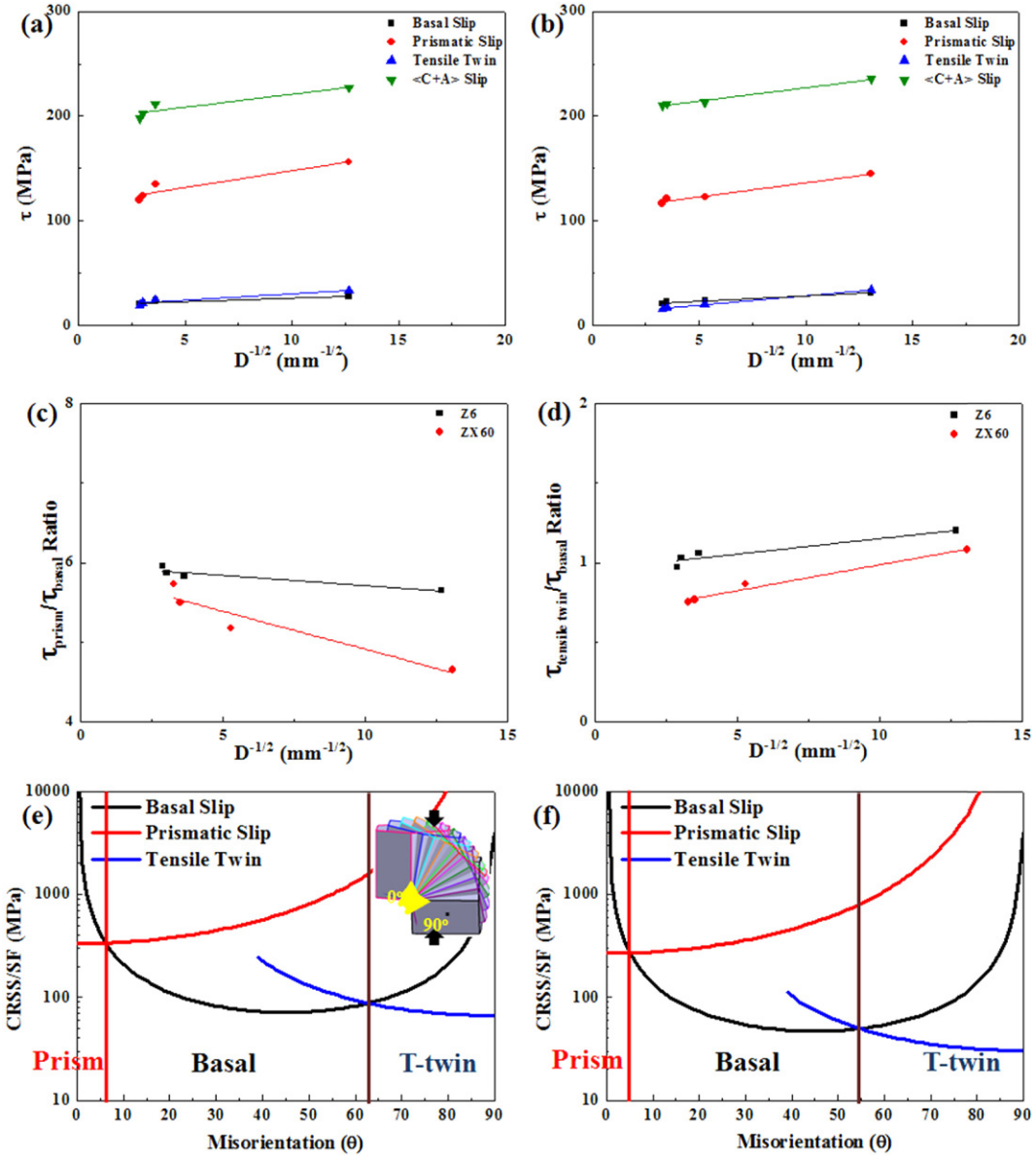

Fig. 2. (a, b) H-P relation of the Z6 and ZX60 calculated by VPSC, (c) CRSS ratios of the prismatic slip modes to the basal slip mode, (d) tensile twin modes to the basal slip mode as a function of grain size, (e, f) stress (CRSS/SF) required to activate the basal, prismatic slip and tensile twin modes for the ZX60 specimens annealed at 350 °C for 1 h and 48 h.

Fig. 2(a), (b) present the Hall-Petch relations of the deformation modes. From the results, an increasing grain size activates more tensile twinning. The slope (k) represents the sensitivity of the grain size. The slope of the tensile twin mode is higher than that of the basal slip mode, which indicates that the tensile twin becomes activated more easily as the grain size increases, given that those values of the two deformation modes are similar (shown in Table 1). The CRSS ratio $\tau_{prism}/\tau_{basal}$ increaseswith increasing grain size, while $\tau_{tensile}/\tau_{basal}$ decreases, which also proves the relationship between tensile twin and grain size in Fig. 2(c), (d). The way to determine the activation of the deformation modes by the CRSS values might not explain all the deformation processes because the VPSC model cannot concern the strain compatibility during the deformations. On the other hand, the CRSS values from VPSC are related to deformation at the early stage, in which strain compatibility are relatively less important. This suggests that more tensile twinning makes the strain compatibility between grains easier due to a decrease in the ratio: $\tau_{tensile\ twin}/\tau_{basal}$. Furthermore, from the (0002) pole figure of the specimens, very little of the grains have a favored orientation for the tensile twin mode. Figure 2(e), (f) shows the stress required (CRSS/Schmid factor) to activate the basal slip, prismatic slip, and tensile twin modes. The CRSS values employed to generate these plots were derived from the VPSC calculations of the ZX60 specimens annealed at 350 ˚C for 1 h and 48 h. A range where the tensile twin mode is favored and increases from a range 62˚ to 90˚ to a range 55˚ to 90˚ with increasing grain size. On the other hand, the range does not include the component in which the maximum intensity is placed. These plots indicate a change in the favored orientation induced by the decrease in $\tau_{tensile\ twin}/\tau_{basal}$. In addition, the roles of tensile twins become more important in ZX60. The slope of the tensile twin in ZX60 has higher k values than that of Z6 and the CRSS ratios of the tensile twin to basal slip ($\tau_{tensile\ twin}/\tau_{basal}$) are lower than those of Z6. A comparison of the CRSS values of deformation modes cannot precisely reflect the deformation behaviors. On the other hand, the coarse grain size and Ca addition reduce the CRSS ratios of the tensile twin to basal slip from the results of the VPSC calculation, which means that these two factors enhance the activation of the tensile twin and improve the stretch formability [5,10,18,19].

EBSD measurements of the Z6 and ZX60 TD planes were taken to investigate the tendency of tensile twinning during the Erichsen tests. Twins are seldom observed in Z6 and ZX60 alloys with finer grain sizes, but many tensile twins form in ZX60 annealed at 350 °C for 1 h (Fig. 3). Although the average grain size of ZX60 is less than half that of Z6, the tensile twins in ZX60 are considerably larger than those in Z6. This also suggests that the enhancement of stretch formability is correlated with the activation of tensile twin. A number of reports have suggested that Ca addition promotes tensile twinning. The effects of alloying elements on tensile twinning are not well established because there are many factors that affect twinning. Shang *et al.* calculated the generalized stacking fault

Table 1. Hall-Petch parameters for Z6 alloys

	Z6		ZX60	
	τ_o (MPa)	k (MPa mm$^{1/2}$)	τ_o (MPa)	k (MPa mm$^{1/2}$)
Basal Slip	19.26	0.66	17.86	1.02
Prismatic Slip	115.51	3.22	109.02	2.71
Tensile Twin	17.98	1.21	10.26	1.79
Pyramidal Slip	195.93	2.49	201.34	2.58

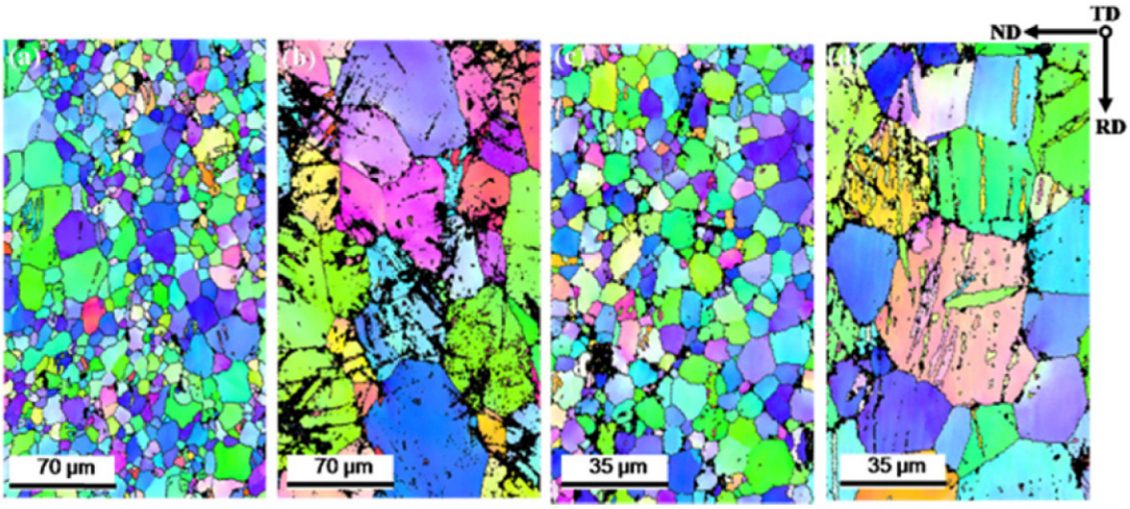

Fig. 3. IPF maps obtained from TD planes of Z6 with (a) Z6 annealed at 250 °C for 1 h, (b) Z6 annealed at 350 °C for 1 h, (c) ZX60 annealed at 250 °C for 1 h, and (d) ZX60 annealed at 350 °C for 1 h.

(GSF) of various Mg alloys and found that the addition of Ca to Mg alloys increased the tensile twinning propensity by the first principle model [9]. Experimental studies showed that the addition of Ca improves the formability of the Mg alloy by activating more tensile twinning [5].

The IE values of the Mg alloys in Fig. 1(a) do not increase in proportion to the grain size. These results indicate that twinning plays a different role in the alloys with coarser grain sizes. The small Erichsen test, in which the size is reduced by one tenth, was carried out to investigate the relationship between deformation twinning and crack formation. The grain orientations of two ZX60 specimens with different grain sizes were observed by EBSD. SEM images were then taken to observe twinning and crack propagation with punch displacements of 1/3 mm and 2/3 mm (Fig. 4). In ZX60 annealed at 350 °C for 1 h, which showed the highest IE value, the cracks initiated at the grain boundaries of the basal planes and propagated along the grain boundaries (see black line in Fig. 4(a)). Cracks did not form near the location of the twins. These results show that twinning enhances the stretch formability of ZX60 alloys. Basal slip mode is activated easily during deformation but it is restricted to the direction of the c-axis. Therefore, tensile twinning may enhance strain accommodation among the grains by releasing the stress concentration. In addition, cracks formed in a different manner in the ZX60 annealed at 350 °C for 24 h (shown in Fig. 4(b)). Most of the cracks shown in Fig. 4(b) also formed at the grain boundaries of the basal planes, but some cracks were found in the inner grains (see the blue circle in Fig. 4(b)). Twinning has been identified as the origin of cracks in the specimens with coarser grain sizes. There is a repulsive interaction between the basal dislocations and tensile twin, which means that a local stress concentration can form via dislocation pile-up at the twin boundaries [18]. Somekawa *et al.* [20] reported that the strain accumulated at the twin boundaries formed cracks that propagated along these boundaries during the fracture toughness tests. Cracks in Z6 also initiated in the grain boundaries of the basal plane but they propagated into the grains unlike in ZX60 (see the blue circle in Fig. 4(c)). The cracks originating in the grain boundaries cut the grains along the <a> direction. A relatively small number of twins appear in the neighboring grains. Like the results of VPSC calculations, Ca addition enhances the activation of tensile twinning, which is likely to play a critical role in releasing the stress concentration on the grain boundaries.

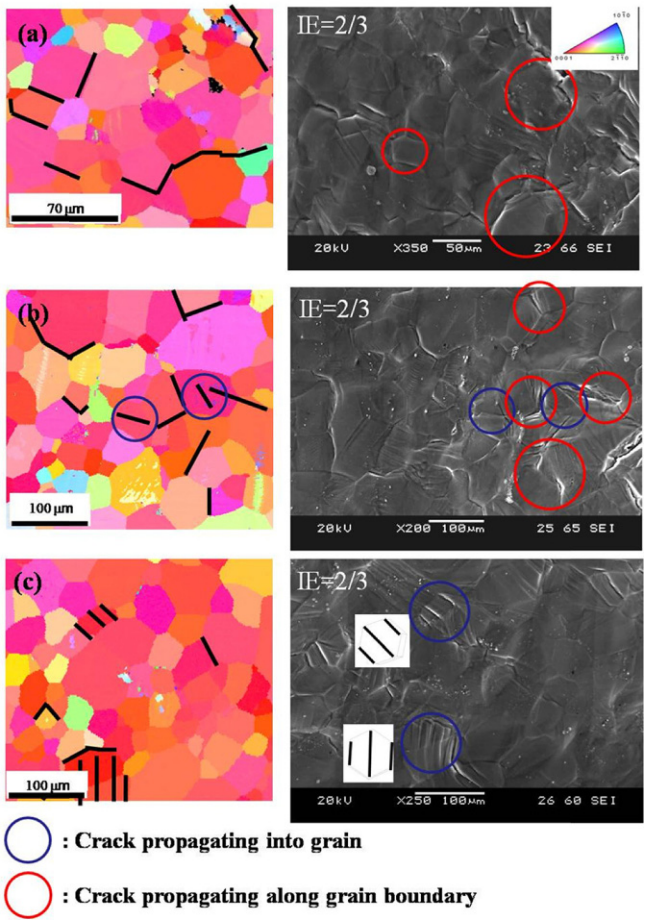

Fig. 4. Origin of crack and propagation during the small Erichsen test: IPF and SEM images of (a, b) ZX60 annealed at 350 °C for 1 h and 24 h, and (c) Z6 annealed at 350 °C for 1 h.

4. CONCLUSION

In the present study, Mg-Zn and Mg-Zn-Ca alloys with various rolling conditions were investigated to disclose the role of tensile twinning on the stretch formability by increasing the grain size and adding Ca. The Ca-containing alloys had a higher IE value, which was associated with twinning. According to VPSC calculations, tensile twining is more prevalent in the specimens with Ca addition and coarse grains. Moreover, as assessed from the EBSD images of Z6 and ZX60 after the Erichsen test, the high IE value is related directly to the propensity of tensile twinning. The IE values of the two alloys increased with increasing grain size up to a certain point and then decreased. The small Erichsen tests were adopted to understand the phenomenon by investigating the twinning behavior during deformation. In ZX60, cracks initiated at the grain boundaries of the basal planes and propagated along the grain boundaries. The results showed that specimens with more tensile twins exhibited high stretch formability corresponding to the EBSD results. On the other hand, some cracks began to occur at the twin boundaries as grain size was increased further, which is caused by the interaction between the tensile twins and basal dislocation, which deteriorates the stretch formability.

ACKNOWLEDGMENT

This study was supported financially by the World Premier Materials (WPM) Program, funded by the Korea Ministry of Knowledge Economy through the Research Institute of Advanced

Materials and the International Research & Development Program of the National Research Foundation of Korea (NRF) funded by the Ministry of Science, ICT &Future Planning (2015R1A2A1A01006795).

REFERENCES

1. S. R. Agnew, M. H. Yoo, and C. N. Tome, *Acta Mater*. **49**, 4277 (2001).
2. M. Yuasa, N. Miyazawa, M. Hayashi, M. Mabuchi, and Y. Chino, *Acta Mater*. **83**, 294 (2015).
3. S. Ando and H. Tonda, *Mater. T. JIM* **41**, 1188 (2000).
4. H. Yan, S. W. Xu, R. S. Chen, S. Kamado, T. Honma, and E. H. Han, *J. Alloy. Compd.* **566**, 98 (2013)
5. B. C. Suh, J. H. Kim, J. H. Hwang, M. S. Shim, and N. J. Kim, *Scientific Reports* **6**, 22364 (2016).
6. J. Y. Lee, Y.-S. Yun, W.-T. Kim, and D.-H. Kim, *Met. Mater. Int*. **20**, 885 (2014).
7. D. W. Kim, B. C. Suh, M. S. Shim, J. H. Bae, D. H. Kim, and N. J. Kim, *Metall. Mater. Trans*. A **44**, 2950 (2013).
8. S. J. Park, H. C. Jung, and K. S. Shin, *Met. Mater. Int*. **22**, 1055 (2016).
9. S. L. Shang, W. Y. Wang, B. C. Zhou, Y. Wang, K. A. Darling, and L. J. Kecskes, *Acta Mater*. **67**, 168 (2014).
10. M. A. Meyers, O. Vohringer, and V. A. Lubarda, *Acta Mater*. **49**, 4025 (2001).
11. M. Z. Bian and K. S. Shin, *Met. Mater. Int*. **5**, 999 (2013).
12. M. R. Barnett, Z. Keshavarz, A. G. Beer, and D. Atwell, *Acta Mater*. **52**, 5093 (2004).
13. Z. R. Zeng, M. Z. Bian, S. W. Xu, C. H. J. Davies, N. Birbilis, and J. F. Nie, *Scripta Mater*. **108**, 6 (2015).
14. J. J. Jonas, S. Mu, T. Al-Samman, G. Gottstein, L. Jiang, and E. Martin, *Acta Mater*. **5**, 2046 (2011).
15. H.-T. Son, Y.-H. Kim, J.-H. Kim, H.-S. Yoo, and J.-W. Choi, *Korean J. Met. Mater*. **53**, 336 (2015).
16. R. Cottam, J. Robson, G. Lorimer, and B. Davis, *Mat. Sci. Eng. A* **485**, 375 (2008).
17. A. Jain and S. R. Agnew, *Mat. Sci. Eng. A* **462**, 29 (2007).
18. Y. Wang and H. Choo, *Acta Mater*. **81**, 83 (2014).
19. K. S. Shin, K. S. Choi, J. H. Hwang, and K. Lee, *Korean J. Met. Mater*. **53**, 569 (2015).
20. H. Somekawa, A. Singh, and T. Mukai, *Phil. Mag. Lett*. **89**, 2 (2009).